

See discussions, stats, and author profiles for this publication at: <http://www.researchgate.net/publication/256328631>

Ligand-Induced Structural Changes in TEM-1 Probed by Molecular Dynamics and Relative Binding Free Energy Calculations

ARTICLE *in* JOURNAL OF CHEMICAL INFORMATION AND MODELING · AUGUST 2013

Impact Factor: 3.74 · DOI: 10.1021/ci400269d · Source: PubMed

CITATION

1

READS

60

4 AUTHORS, INCLUDING:



João Miguel Martins

University of Copenhagen

9 PUBLICATIONS 42 CITATIONS

[SEE PROFILE](#)



Rúben Fernandes

Polytechnic Institute of Porto

30 PUBLICATIONS 131 CITATIONS

[SEE PROFILE](#)



Irina Moreira

University of Coimbra

50 PUBLICATIONS 1,110 CITATIONS

[SEE PROFILE](#)

Ligand-Induced Structural Changes in TEM-1 Probed by Molecular Dynamics and Relative Binding Free Energy Calculations

A. C. Pimenta,^{†,‡,§} J. M. Martins,[†] R. Fernandes,^{‡,§} and I. S. Moreira^{*,†}

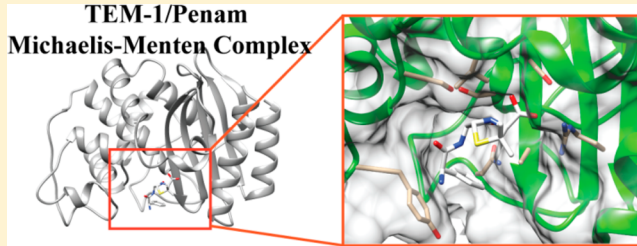
[†]REQUIMTE/Departamento de Química, Faculdade de Ciências da Universidade do Porto, Rua do Campo Alegre s/n, 4169-007 Porto, Portugal

[‡]Centro de Investigação em Saúde e Ambiente, da Escola Superior de Tecnologia da Saúde do Porto, do Instituto Politécnico do Porto, Rua Valente Perfeito 322, 4400-330 Vila Nova de Gaia, Portugal

[§]Centro de Farmacologia e Biopatologia Química (U38-FCT), Faculdade de Medicina da Universidade do Porto, Alameda Prof. Hernâni Monteiro, 4200-319 Porto, Portugal

Supporting Information

ABSTRACT: The TEM family of enzymes has had a crucial impact on the pharmaceutical industry due to their important role in antibiotic resistance. Even with the latest technologies in structural biology and genomics, no 3D structure of a TEM-1/antibiotic complex is known previous to acylation. Therefore, the comprehension of their capability in acylate antibiotics is based on the protein macromolecular structure uncomplexed. In this work, molecular docking, molecular dynamic simulations, and relative free energy calculations were applied in order to get a comprehensive and thorough analysis of TEM-1/ampicillin and TEM-1/amoxicillin complexes. We described the complexes and analyzed the effect of ligand binding on the overall structure. We clearly demonstrate that the key residues involved in the stability of the ligand (hot-spots) vary with the nature of the ligand. Structural effects such as (i) the distances between interfacial residues (Ser70–Oγ and Lys73–Nζ, Lys73–Nζ and Ser130–Oγ, and Ser70–Oγ–Ser130–Oγ), (ii) side chain rotamer variation (Tyr105 and Glu240), and (iii) the presence of conserved waters can be also influenced by ligand binding. This study supports the hypothesis that TEM-1 suffers structural modifications upon ligand binding.



INTRODUCTION

In the 21st century, infectious diseases are a major concern in public health, in great part, due to the increasing capability of pathogens to resist the antibiotics used in clinical practice.¹ Not only have resistance mechanisms to new antibiotics appeared but also the capability of the microorganisms to resist antibiotics has spread.² These facts are of such importance that the screening of resistant or multiresistant microorganisms is performed in several countries. In Gram-negative pathogens, the most common mechanism of resistance is the production of enzymes capable of hydrolyzing antibiotics—β-lactamases.³ These enzymes are screened worldwide, and an online database is readily accessible.⁴ Among these enzymes, a very important family is the TEM family of β-lactamases, which can present different acylating capabilities and therefore different phenotypes (i.e., ESBL,^{1,5} IRT,^{6,7} and CMT^{8,9}). A general 3D structure can be appointed and is formed by three main domains organized as sandwich-like—α-helix/β-sheets/α-helix.

The ability of an enzyme to bind to a ligand is strongly determined by the tridimensional structure of both molecules. Therefore, the ability to determine their structure is crucial to a better prediction and understanding of complex formation. The advances in technologies in structural genomics¹¹ and biology,¹² such as protein expression and purification, microcrystallization,

the use of synchrotrons,¹⁴ and the increasing automation of all the processes, made possible an exponential increase in the number of biomacromolecules with a known tridimensional (3D) structure. Even though macromolecular structures are often used to study biochemical processes, they still present some important limitations. These static structures only represent one possible conformation (X-ray) or a limited ensemble (NMR—Nuclear Magnetic Resonance) that correspond to the structures that are more stable under the conditions of the experiments.¹⁵ However, when analyzing macromolecules (i.e., proteins), their flexibility should be taken into account.^{15–17} Enzymatic studies have an extra challenge, which is the difficulty associated with obtaining a 3D structure of the complex, either due to the kinetic properties of the enzyme (reaction occurs too rapidly to obtain a protein/ligand complex) or due to the instability of the complex itself. When it is possible to obtain the 3D structure of the complex, it remains important to take into account the inherent structural variations, which can be done by Molecular Dynamic (MD) simulations.^{15,18,19} By performing this type of simulation, we can analyze the structural variation of the individual molecules and study the effect of ligand binding into the enzymatic

Received: May 7, 2013



ACS Publications

© XXXX American Chemical Society

A

dx.doi.org/10.1021/ci400269d | J. Chem. Inf. Model. XXXX, XXX, XXX–XXX

structure. MD simulations have been successfully performed to simulate biological properties, and the number of studies using this methodology increases.^{19–26} MD simulations also take into account the role of the solvent in the proteins structural variations and in the ligand geometry.¹⁸

The TEM family of enzymes has been heavily studied due to their importance in antibiotic resistance. However, despite great efforts, a 3D structure of a TEM/antibiotic complex preacylation has not yet been obtained through structural biology methods. The ability of the enzymes to quickly acylate the antibiotics may be the reason. This limitation led to the necessity of studying the antibiotic resistance promoted by these enzymes (i.e., kinetic data and results from disc diffusion methods) from the 3D structure of the protein uncomplexed. Although good results have been obtained by several authors,^{6,27–29} the molecular structure of the protein upon ligand binding cannot be analyzed. This limitation is of special importance when (i) trying to justify differences observed in the kinetic properties and (ii) studying the catalytic reaction, as residues that intervene in ligand binding or stabilization or in the proton transfer network cannot be analyzed properly. Molecular docking methodologies allow us to overcome these limitations, especially when using algorithms that take into account the flexibility of both the protein and ligand.^{18,30,31} These methodologies along with MD simulations and relative free energy calculations grant the capability to analyze complexes more thoroughly.^{32–34} In this work, the complexes between TEM-1 and ampicillin or amoxicillin are characterized. A detailed description of their protein/ligand interface is made. Hot-spots (HS), residues that upon alanine mutation generate a binding free energy difference higher than 2.0 kcal/mol,³⁵ are identified. Interatomic contacts are calculated, and the presence of water molecules near interfacial residues is depicted. A comparison between the structure of the protein uncomplexed and in complex with two small molecules is made to study the conformational rearrangements of the TEM-1 structure caused by ligand binding.

METHODOLOGY

Structure Preparation. The protonation states of TEM-1 (PDB ID: 1ZG4¹⁰) were assigned by EPIK³⁶ in MAESTRO—Schrödinger Software, LLC (see Figure 1).³⁷ All residues were found at their physiological protonation state.

TEM-1 Molecular Dynamics Simulation. TEM-1 was stabilized and refined by MD simulation with the modified

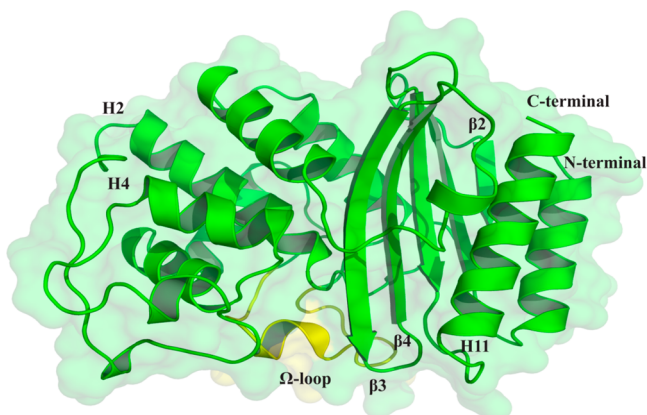


Figure 1. Structural representation of TEM-1 (PDB ID: 1ZG4¹⁰) with some of the key secondary structures identified.

Cornell force field, by Duan et al.—ff03.^{38,39} The MD simulation was carried out in explicit solvent with the TIP3P (79) water model using the AMBER9 program. Seven Na⁺ counterions were added to keep the whole system neutral and a 10 Å separation between each edge of the box and the closest solute atom was used to minimize electrostatic interactions between periodic images of the solute. First, the water was equilibrated in the presence of the fixed complex (25 ps); then only the side chains were relaxed (200 ps)—minimization, and finally a production run of 16 ns was done for the system. During the initial 2 ns of the production run, the temperature was increased from 0 to 300 K followed by 48 ns of production at a constant 300 K (ensemble NPT) using a “weak-coupling” barostat (Berendsen barostat).⁴⁰ In the restrained simulations, the atoms were subjected to a harmonic restraining force of 10 kJ mol⁻¹ nm⁻². In all MD simulations, the bond lengths involving hydrogens were constrained using the SHAKE algorithm.⁴¹ The equations of motion were integrated with a 2 fs time step, and the Langevin algorithm^{42,43} was used to regulate the temperature of the system. All of the crystallographic waters were removed from the structure subjected to the MD simulation. Periodic boundary conditions were applied using PME^{44,45} to treat long-range electrostatic interactions. After establishing the stability of the MD simulation, we have calculated the RMSD (Root-Mean-Square-Deviation) to the average structure and selected six structures with the lowest value. These six structural representatives of the ensemble generated for the wild-type were used in the following procedure: protein–ligand docking.

Molecular Docking. Protein–ligand docking was performed using the six microstates ensemble from the protein MD simulation as targets and the penicillins: amoxicillin and ampicillin. The selection of these antibiotics was based on the facts that they are known substrates of penicillinases like TEM-1⁴⁶ and are widely used in clinical practice.⁴⁷ Their structures were obtained from PubChem Compound.⁴⁸ The AutoDock 4.2 package⁴⁹ was used for the entire docking procedure. An energy grid of 46 Å × 40 Å × 40 Å in dimensions, with a 0.375-Å grid spacing (the center of the Grid Box and dimension were previously tested), was generated with the program AutoGrid. Gasteiger charges were assigned to the ligand atoms. AutoDock 4 was used to evaluate ligand-binding energies over the conformational search space using the genetic algorithm-local search method. Default docking parameters were used with the following exceptions: ga-pop-size, 200; ga-num-evals, 10 000 000; and ga-run, 50. The structural poses that resulted from the docking were analyzed taking into account several parameters: (i) The binding energy should be negative. (ii) The complexes should have low energy and form clusters with a higher number of complexes. (iii) The β-lactam ring should be on the more internal part of the catalytic pocket and, if possible, facing the catalytic Ser70. (iv) The complexes should have a high number of interactions (protein–ligand).

Molecular Dynamics Simulation of the Protein–Ligand Complexes. The final complexes obtained from the molecular docking were stabilized and refined by MD simulations following the procedure described in the TEM-1 Molecular Dynamics Simulation section. To obtain the parameters for amoxicillin and ampicillin, partial atomic charges were derived with the standard HF/6-31G* RESP⁵⁰ (Tables S1 and S3 in Supporting Information) methodology using the program Antechamber implemented in the Amber package.⁵¹ Atom types and missing force-field parameters of the ligands (Tables S2 and S4 in the Supporting Information) were assigned with the GAFF force

field.⁵² Although the ligand parametrization can be challenging, this was not the case as our organic compounds are composed by some of the most common atoms present in the organic chemical space (C, N, O, S, H) in a typical spatial arrangement (chemical structures of amoxicillin and ampicillin shown in Figures S1–S3 in the Supporting Information).

Structural Analysis. RMSDs of the protein backbone, amoxicillin, and ampicillin were calculated for all the MD simulations in order to investigate their stability. For a detailed study of the binding interface, significant residues were selected: Met69, Ser70, Lys73, Tyr105, Ser130, Asn132, Glu166, Asn170, Val216, Lys234, Ser235, Glu240, Arg244, and Arg275. This selection took into account the literature^{5,53,54} to ensure that crucial residues were selected. For these residues, B-factors were calculated to investigate the deviation of these compared to a reference position. The environment around the same residues was carefully characterized. For this step, all residues and water molecules within 5 Å of each interfacial residue were selected, and their occupancy was estimated. We have also analyzed the radial distribution function, $g(r)$ or RDF, as well as the average number of waters within a given distance of all interfacial residues. $g(r)$ gives the probability of finding an atom at distance r from another atom, in relation to the probability expected for a bulk solvent distribution at the same density. It was calculated by compiling a histogram with a spacing of 0.02 and a range of 8 Å. These two procedures as well as the visual inspection of the MD simulations were performed with the VMD package and tailor-made scripts.⁵⁵ Crucial interatomic distances for the enzyme catalytic activity and enzymatic inhibition were measured for all the MD simulations. All structural representations were made by the PYMOL package.⁵⁶

Energetic Profile. The MM-PBSA (Molecular Mechanics Poisson–Boltzmann Surface Area) script⁵⁷ integrated into the AMBER 9 package⁵⁸ was used to calculate the binding free energy difference upon alanine mutation. The alanine mutations were performed on the interface residues that were previously selected in the structural analysis with the exception of alanine, glycine, or proline residues. These were not mutated since they usually have a primary role in the protein stability and the mutation could lead to protein degradation. Due to the limitations of the method, residues that would only interact *via* backbone could not be analyzed with computational Alanine Scanning Mutagenesis (ASM). This method combines a continuum approach to model solvent interactions with a MM-based approach to atomistically model protein–protein interactions. It provides speed and accuracy and has been used quite a bit in past years.^{20,22,57,59–70} The MM-PBSA approach first developed by Huo et al.⁵⁷ was improved by Moreira et al.⁶² and can now be applied with an accuracy of 1 kcal/mol. The mutant complexes are generated by a single truncation of the mutated side chain, replacing C γ with a hydrogen atom and setting the C β –H direction to that of the former C β –C γ . For the binding energy calculations, a total of 25 snapshots of the complexes were extracted in the last 1 ns of the run. The $\Delta\Delta G$ is defined as the difference between the mutant and wild type complexes defined as

$$\Delta\Delta G = \Delta G_{\text{cpx-mutant}} - \Delta G_{\text{cpx-wild type}} \quad (1)$$

Typical contributions to the free energy include the internal energy (bond, dihedral, and angle), the electrostatic and the van der Waals interactions, the free energy of polar solvation, the free energy of nonpolar solvation, and the entropic contribution:

$$\begin{aligned} G_{\text{molecule}} &= E_{\text{internal}} + E_{\text{electrostatic}} + E_{\text{vdW}} + G_{\text{polar-solvation}} \\ &+ G_{\text{non-polar-solvation}} - TS \end{aligned} \quad (2)$$

For the calculations of relative free energies between closely related complexes, it is assumed that the total entropic term in eq 2 is negligible as the partial contributions essentially cancel each other.⁶⁷ The first three terms of eq 2 were calculated with no cutoff. The $G_{\text{polar-solvation}}$ was calculated by solving the Poisson–Boltzmann equation with the software DELPHI.^{71,72} In this continuum method, the protein is modeled as a dielectric continuum of low polarizability embedded in a dielectric medium of high polarizability. We used a set of values for the DELPHI parameters that have been proven in a previous study to constitute a good compromise between accuracy and computing speed.⁷³ We used a value of 2.5 grids/Å for scale (the reciprocal of the grid spacing), a value of 0.001 kT/c for the convergence criterion, 90% for the fill of the grid box, and the Coulombic method to set the potentials at the boundaries of the finite-difference grid. The dielectric boundary was taken as the molecular surface defined by a 1.4 Å probe sphere and by spheres centered on each atom with radii taken from the Parse⁷⁴ vdW radii parameter set. The key aspect of the new improved approach is the use of a three dielectric constant set of values ($\epsilon = 2$ for nonpolar residues, $\epsilon = 3$ for polar residues, and $\epsilon = 4$ for charged residues plus histidine) to mimic the expected rearrangement upon alanine mutation (the method is described in refs 60 and 62). It is important to highlight that we used only one trajectory for the computational energy analysis, as it has been proven to give the best results.⁶² Side-chain reorientation was implicitly included in the formalism by raising the internal dielectric constant. The nonpolar contribution to the solvation free energy due to van der Waals interactions between the solute and the solvent was modeled as a term dependent on the solvent accessible surface area (SASA) of the molecule. It was estimated using empirical parameters derived from experimental transfer energies of hydrocarbons:^{57,74} 0.00542 kcal/Å² mol × SASA + 0.92 kcal/mol. The SASA was determined using the molsurf program, which computes the molecular surface defined by Connolly.⁷⁵ The PROBIS⁷⁶ server was also used to detect the structurally similar binding sites in TEM-1.

RESULTS

Docking Protein–Ligand. *1. Enzymatic Ensemble.* To inquire about the stability of the protein through the MD simulation, the RMSD was calculated for the protein backbone. The RMSD presented in Figure 2 is always lower than 1.6 Å, showing that the MD simulation is very stable. We have also highlighted that the variance along the MD simulation never surpasses 0.7 Å.

2. Organic Compounds/TEM-1 Docking. To better analyze the protein–ligand docking results, it would have been beneficial to have an X-ray structure of a TEM enzyme in complex with some of the chosen antibiotics. However, as stated in the Introduction, there is not a 3D structure of the TEM enzyme complexes with these antibiotics, previously to acylation. Nevertheless, complexes were found with TEM variants and different antibiotics: intermediates of the catalytic reaction complexes (i.e., PDB ID: 1FQG,⁷⁷ 1TEM,⁷⁸ and 1BT5⁷⁹). Given these shortcomings, the structural poses that resulted from the docking procedures were analyzed with several parameters as previously described in the Molecular Docking section. TEM-1 formed complexes (Supporting Information, Figure S4) with

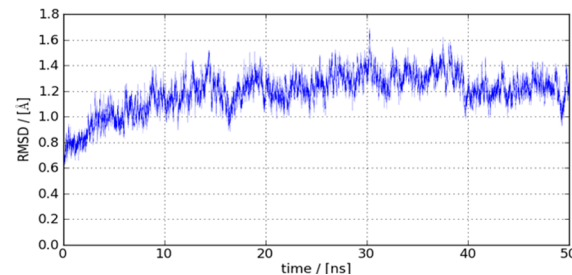


Figure 2. Graphical representation of the RMSD of the backbone of TEM-1.

both the ligands (ampicillin and amoxicillin), and the structures of the antibiotic chains are very similar to the one found for 1FQG⁷⁷ (complex between a TEM variant and penicillin G).

Molecular Dynamics—Structural and Energetic Analysis. With the aim of rationalizing the binding mode of the various compounds inside the binding pocket of the TEM-1 as well as the conformational changes induced by the binding of the ampicillin and amoxicillin, we performed 50 ns MD simulations of the two complexes and of TEM-1 uncomplexed.

1. Structural Stability during the MD Simulations. The RMSDs of the backbone with respect to the initial structures were calculated along the MD to assess the stability of the two complexes and TEM-1 uncomplexed. The complex TEM-1/ampicillin (Figure 3a) presents a very stable backbone of the

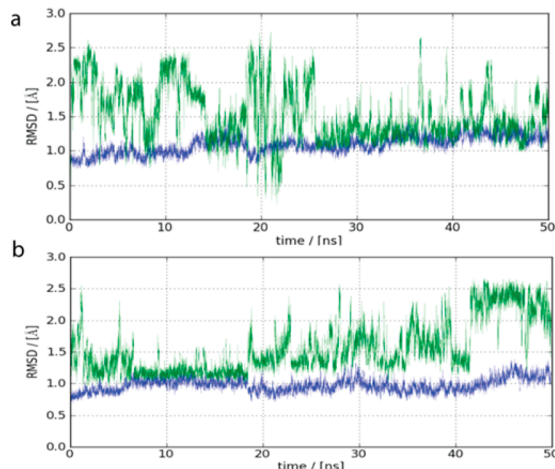


Figure 3. Graphic representation of the RMSDs of TEM-1 in complex with ampicillin (a) and amoxicillin (b). In blue and green are the RMSDs for the protein backbone and the antibiotics, respectively.

protein, but some variance can be observed on the ligand's geometry—side chain movement, which results in the RMSD variation observed for ampicillin along the MD simulation. The complex TEM-1/amoxicillin (Figure 3b) presents a good stability for both the ligand and the protein up to 20 ns, at which point the side chain of amoxicillin presents a slight movement toward β 3 and H11.

2. Structural and Energetic Profiling. Given the complexity of the reactions involved in the hydrolysis and inhibition of this class of enzymes, and since the stability of a ligand does not necessarily translate into degradation/enzyme inhibition, it is not adequate to rely only on the absolute binding free energy ($\Delta G_{\text{binding}}$) to distinguish the capacity of the organic compounds. It is well-known that the reaction of acylation of the β -lactam ring

does not involve only the catalytic residues but also a complex network of H-bonds that lead to an abstraction of a hydrogen of the catalytic serine residue (Ser70) leading to the nucleophilic attack of Ser70 to the β -lactamic ring (carbonyl group).^{80–82} Two distinct theories have been proposed (Supporting Information Scheme 1): (i) Glu166 might be the initial reaction base residue (after the abstraction of a hydrogen by a water molecule), abstracting a hydrogen from Lys73, which would then abstract the hydrogen from the hydroxyl group of the Ser70.²⁷ (ii) Glu166 acts as the initial base abstracting a hydrogen from Ser70 mediated by a highly conserved water molecule and Ser130 acting as a catalytic acid donating a hydrogen to the nitrogen atom of the β -lactamic ring.⁸¹ Lys73 has been described not only as a possible initial base but also as a stabilizer of nearby residues (Ser130 and Ser70) and as having a possible stabilizing effect as far as ligand position goes. Other theories have arisen with the study of various TEM variants, and it has been proposed that Lys73 might be, in certain cases, the initial base residue.^{82,83} Although the importance of these residues was shown, the definite purpose of some of them and how they might influence the reactions on the catalytic site are not clear. So, it becomes necessary to take into account several aspects of the enzyme itself and the complexes formed for a correct comprehension of these crucial systems.

To analyze the structure of the complexes and TEM-1 alone, more specifically the residues near the catalytic pocket, B-factor values to describe the displacement of the atomic positions from an average value (Table 1) were calculated. B-factor values for the

Table 1. B-Factors Values of the Interfacial Residues: for the Backbone (BB) and for All-Atom (AA)

residues	B-factor					
	TEM-1					
	ampicillin		amoxicillin		uncomplexed	
residues	BB	AA	BB	AA	BB	AA
Met69	10.94	21.64	6.84	10.27	6.22	7.44
Ser70	9.09	11.98	5.56	16.58	6.96	13.46
Lys73	5.56	7.34	4.12	8.29	3.69	5.19
Tyr105	33.91	96.47	17.84	45.01	11.70	67.00
Ser130	7.55	11.13	10.52	14.85	4.57	6.03
Asn132	5.59	11.96	7.04	19.63	3.74	11.34
Glu166	11.12	20.70	8.83	21.37	8.14	17.74
Asn170	12.40	37.50	9.91	24.02	8.04	10.38
Val216	25.75	38.61	19.41	32.80	8.22	11.04
Lys234	14.08	19.45	4.47	8.192	3.52	4.97
Ser235	8.82	22.78	6.88	11.62	5.64	8.62
Glu240	9.54	26.76	8.09	23.05	60.32	239.27
Arg244	5.05	18.16	8.36	15.92	3.90	7.32
Arg275	10.17	12.05	11.34	14.56	8.80	17.06

backbone of all residues of TEM-1 when in complex or uncomplexed are shown in Figure 4 along with the B-factor values obtained from the TEM-1 structure PDB ID 1ZG4.²⁷ This graphical representation allows a qualitative comparison between the protein structures of the MD simulations as performed by Bren and Oostenbrink.⁸⁴ It is noticeable that the backbone of the protein presents similar variance profiles, which are also similar to the profile obtained from the crystallographic structure. Three main differences between the calculated B-factor for TEM-1 alone and the values from the crystallographic structure are found (Ile173, Gly236, and Pro252 residues). Glycine and proline

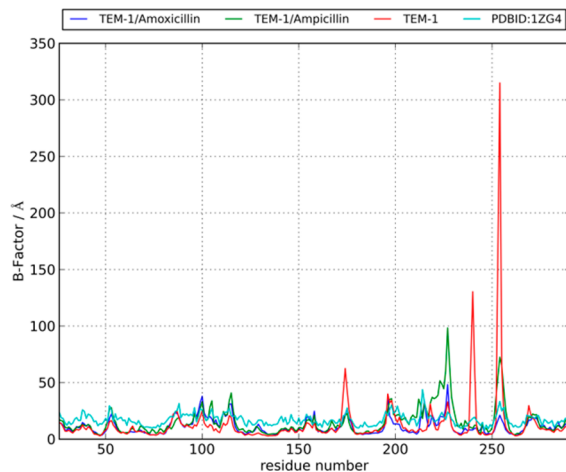


Figure 4. Graphical representation of the TEM-1's backbone B-factor in complex with amoxicillin (blue) and ampicillin (green), in an uncomplexed MD (red) and in the X-ray structure (PDB ID: 1ZG4²⁷; cyan).

residues can cause great variability in the protein structure, and in TEM-1 Pro252 is located in the loop at the end of β 4 and Gly236 is located at the end of β 3 near the β 3– β 4 loop. Loops have been described as the most variable regions in TEM-1 in MD simulations.²⁴ Although the greater variances in stability are observed for the side chains and the variability profiles are similar, it is possible to see several important structural differences when comparing this enzyme uncomplexed or in complex with the antibiotics. The stability of the residues near the catalytic pocket is affected upon ligand binding, and it can diverge depending on the ligand itself. The calculated B-factor values for Glu240 clearly demonstrate this fact. The side chain shows higher B-factor values when not in a complex form, and this might be the result of a lack of key interactions that appear upon complex formation. This would also justify why the B-factor value for Glu240 is much higher in TEM-1 uncomplexed than in the complexes (values for backbone and all atom are similar in the complexes, while for TEM-1 it is significantly higher, 60.32 for backbone and 239.27 for all atoms).

The number of water molecules (Table 2) was also calculated to investigate the presence of water molecules near the catalytic

Table 2. Number of Water Molecules at 4 Å in the Micro-Environment of the Interfacial Residues

residues	number of water molecules		
	ampicillin	amoxicillin	uncomplexed
Met69	2.40	2.42	0.00
Ser70	2.03	1.39	2.79
Lys73	1.38	0.68	1.01
Tyr105	0.14	0.46	2.48
Ser130	1.66	1.88	0.79
Asn132	0.94	1.93	1.91
Glu166	0.24	0.18	1.02
Asn170	1.10	0.74	1.67
Val216	0.59	0.80	2.03
Lys234	1.65	1.71	2.49
Ser235	1.13	1.12	3.02
Glu240	0.04	0.00	5.37
Arg244	0.02	0.33	3.28
Arg275	3.05	1.37	3.23

residues as well as others that might contribute to the stability of the complex. It also allowed a better comprehension of the capability of the enzymes to hydrolyze the antibiotics. Although out of the scope of this work, the molecular interactions involved in hydration could be described in more detail with the protocol developed by Bren et al.^{85,86} via RDF measurements. By increasing rotational and translational temperatures, each term (i.e., vdW, electrostatic) could be analyzed taking into account the type of molecule hydrated (polar, ionic, or neutral) and the specific interactions (H-bonds, repulsive Pauli forces, ion–dipole interactions, and attractive dispersion interactions).

The number of water molecules around the interfacial residues presents a different behavior upon complex formation and also between the two complexes. In both preacylation complexes, the conserved water molecule that is H-bonded to Glu166 and Ser70 in TEM-1 uncomplexed and that has been identified in post-acylation complexes suffers a displacement. The reason for this difference might be the displacement of the intact structure of the antibiotics, mainly the bicyclic structure that forms the core of the antibiotic, into the catalytic site. The closed form of the antibiotic occupies a larger volume in comparison to the open structure formed upon acylation. The structure of a TEM variant with other penam has been obtained thorough crystallography (PDB ID: 1FQG⁷⁷). This is a structure obtained after the acylation and consequent ring-opening of the antibiotic, which is therefore covalently bonded to the enzyme. These post-acylation characteristics led to a different position and orientation of the ligand within the catalytic pocket, and also since the bicyclic structure is opened, the bulk inside the catalytic pocket has been reduced, leaving more space available for the presence of water molecules between Glu166 and Ser70. These might explain why the conserved water molecule has been displaced in the Michaelis–Menten intermediates. Tyr105 presents fewer water molecules when TEM-1 is in complex with amplicillin and amoxicillin (0.14 and 0.46, respectively) than for TEM-1 uncomplexed (2.48). These results can be explained by the interaction of Tyr105 with amplicillin and amoxicillin that protects the ligands from the bulk solvent and stabilizes them within the catalytic pocket. Figure 5b and c illustrate the general orientation and position of the two ligands in a representation of the MD simulations. It can be perceived that they are in accordance with the crystallographic structure of the post-acylation complex, as it is possible to see that both side chain and bicyclic structures of amplicillin and amoxicillin are lowered and occupy greater volume within the catalytic pocket. The space between Glu166 and Ser70 is occupied by the bicyclic structure of the antibiotic, which does not happen with the open ring of the post-acylation penam of 1FQG.²⁷

We also performed a computational ASM for a better comprehension of the role of the various residues within the binding pocket. A computational ASM of a protein–ligand interface has already been shown to be efficient.^{77,87} In Tables 3 and 4 are listed the decomposition of the free binding energy into its additive contributions, adequately representing the system with the sum of its contributions. Such decomposition is usually performed with the free energy perturbation methodology and allows for the depiction of the most significant interactions between complexes' molecules providing structure/activity relationships.⁸⁸ The comprehension of such properties can be used as a foundation in methodologies within the field of drug design, such as molecular docking scoring.⁸⁹ The complex TEM-1/ampicillin presents eight HSs: Met69 ($\Delta\Delta G_{\text{binding}} = 8.06 \pm 1.30 \text{ kcal mol}^{-1}$), Ser70 ($\Delta\Delta G_{\text{binding}} = 2.99 \pm 0.96 \text{ kcal mol}^{-1}$),

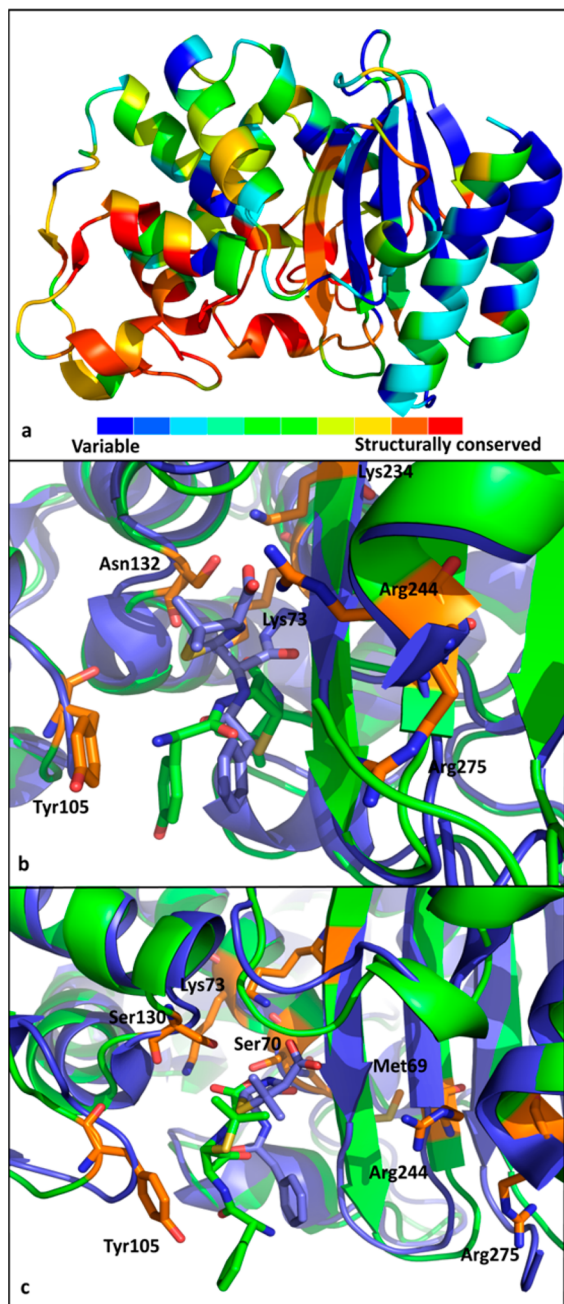


Figure 5. Structural representations of TEM-1: (a) colored by structural conservation using the PROBIS⁷⁶ server with PDB ID 1ZG4²⁷ as a template; in complex with (b) amoxicillin and (c) ampicillin. Then, MD representative structures are colored in green and the TEM-1 structure in blue (PDB ID: 1FQG⁷⁷) with HS highlighted in orange.

Lys73 ($\Delta\Delta G_{\text{binding}} = 16.48 \pm 0.84 \text{ kcal mol}^{-1}$), Tyr105 ($\Delta\Delta G_{\text{binding}} = 8.17 \pm 0.99 \text{ kcal mol}^{-1}$), Ser130 ($\Delta\Delta G_{\text{binding}} = 2.25 \pm 0.87 \text{ kcal mol}^{-1}$), Lys234 ($\Delta\Delta G_{\text{binding}} = 11.89 \pm 0.85 \text{ kcal mol}^{-1}$), Arg244 ($\Delta\Delta G_{\text{binding}} = 6.96 \pm 0.86 \text{ kcal mol}^{-1}$), and Arg275 ($\Delta\Delta G_{\text{binding}} = 4.50 \pm 0.86 \text{ kcal mol}^{-1}$). The major contributions for the relative binding free energy of the positively charged residues (lysine and arginine), serine, and Met69 residues are electrostatic interactions. The importance of these contributions is explained by the interaction with the carboxylic group of ampicillin and amoxicillin. The major contributions for the relative free binding energy of Tyr105 are hydrophobic interactions of the side chain of Tyr105 with the ring of ampicillin

($\Delta\Delta E_{\text{VDW}} = 5.12 \pm 1.35 \text{ kcal mol}^{-1}$)— π – π stacking—and electrostatic interactions ($\Delta\Delta E_{\text{Ele}} = 5.29 \pm 1.27 \text{ kcal mol}^{-1}$). The complex TEM-1/amoxicillin presented six HSs: Lys73 ($\Delta\Delta G_{\text{binding}} = 14.93 \pm 0.71 \text{ kcal mol}^{-1}$), Tyr105 ($\Delta\Delta G_{\text{binding}} = 2.36 \pm 0.85 \text{ kcal mol}^{-1}$), Asn132 ($\Delta\Delta G_{\text{binding}} = 3.00 \pm 0.94 \text{ kcal mol}^{-1}$), Lys234 ($\Delta\Delta G_{\text{binding}} = 7.42 \pm 0.70 \text{ kcal mol}^{-1}$), Arg244 ($\Delta\Delta G_{\text{binding}} = 4.47 \pm 0.72 \text{ kcal mol}^{-1}$), and Arg275 ($\Delta\Delta G_{\text{binding}} = 3.23 \pm 0.72 \text{ kcal mol}^{-1}$). Tyr105 stabilizes the lateral side chain of the antibiotic with hydrophobic interactions (π – π stacking) of the two rings involved, leading to a high contribution of the van der Waals energy ($\Delta\Delta E_{\text{VDW}} = 3.03 \pm 0.89 \text{ kcal mol}^{-1}$). Other residues have been identified as important contributors for the ligand stabilization (but less efficient): Ser70 ($\Delta\Delta G_{\text{binding}} = 1.57 \pm 0.85 \text{ kcal mol}^{-1}$) and Asn170 ($\Delta\Delta G_{\text{binding}} = 1.91 \pm 0.87 \text{ kcal mol}^{-1}$). Lys73 and Ser70 have also been identified as determinant residues in the stabilization of ampicillin, confirming that these residues are important for the acylation reaction, not only due to its capability to shuttle protons and perform nucleophilic attack but also by stabilization of the bicyclic structure of the antibiotic (ampicillin). In the TEM-1/amoxicillin complex, Lys73 shows a great ligand stabilization effect as in TEM-1/ampicillin, but the effect of Ser70 is less pronounced. In accordance with the results for TEM-1/ampicillin complex, positively charged residues present a great electrostatic contribution to the relative free binding energy due to the interaction with the acidic group of amoxicillin. In both complexes, Arg275 has been detected as HS due to its electrostatic contributions: We have to highlight that Arg275 has the ability to change between rotamers, allowing its side chain to be in different distances related to the antibiotic. In both complexes, Arg275 has lower relative free binding energy than Arg244, as the latter is closer to the ligand. Although Ala237 cannot be tested using computational ASM, it was a key component for the stabilization of the substituents of the bicyclic structure of ampicillin. These results are in accordance with the O-ring theory that proposes the inaccessibility of a residue to solvent as a determinant factor for the residue to become a HS.^{61,69,90,91} Figure 5a illustrates the results obtained with the PROBIS⁷⁶ server where the structural conservation is represented by a color gradient. This server allows the detection of structurally similar binding sites in the PDB without reference to known binding sites or cocrystallized ligands and takes into account entire protein surfaces. It is noticeable that residues identified as HS are primarily located in highly conserved regions colored as yellow and red (i.e., Lys73 and Tyr105), and even HSs identified in regions of greater structural variability such as Arg244 and Arg275 present greater conservation than the remaining residues in the same secondary structures. These results suggest that structural conservation algorithms can be used to predict important residues in ligand binding in accordance with the results from Nejc et al.⁹²

To investigate if the H-bond network between the catalytic residues is maintained through the MD simulation, relevant distances were also calculated (Table 5).

The distances measured between key residues have also shown that the ligands influence the position of the side chain of the residues near the catalytic pocket. When in complex, TEM-1 presents a significant increase for the distance between Ser70–O γ and Lys73–N ζ (average of $3.18 \pm 0.75 \text{ \AA}$ in TEM-1 uncomplexed, $4.54 \pm 1.31 \text{ \AA}$ in TEM-1/amoxicillin, and $5.96 \pm 1.04 \text{ \AA}$ in TEM-1/ampicillin). This can hinder the proton transfer between these residues. Nevertheless, it can still occur as these side-chains were also found to be closer in the TEM-1/ampicillin complex (8.5% of the time they are closer than 4 \AA). In

Table 3. Decomposition of the Relative Binding Free Energy upon Computational ASM for Complex TEM-1/Ampicillin

residues	ampicillin/[kcal mol ⁻¹]				
	$\Delta\Delta E_{\text{Ele}} \pm \text{SD}$	$\Delta\Delta E_{\text{VDW}} \pm \text{SD}$	$\Delta\Delta G_{\text{nonpolar-solvation}} \pm \text{SD}$	$\Delta\Delta G_{\text{polar-solvation}} \pm \text{SD}$	$\Delta\Delta G_{\text{binding}} \pm \text{SD}$
Met 69	8,02 ± 1,90	0,08 ± 1,33	0,00 ± 0,08	-0,04 ± 1,17	8,06 ± 1,30
Ser 70	7,33 ± 1,22	-1,85 ± 1,29	-0,01 ± 0,08	-2,48 ± 0,75	2,99 ± 0,96
Lys 73	17,29 ± 0,82	0,55 ± 1,33	0,00 ± 0,08	-1,36 ± 0,61	16,48 ± 0,84
Tyr 105	5,29 ± 1,27	5,12 ± 1,35	0,46 ± 0,09	-2,70 ± 0,71	8,17 ± 0,99
Ser 130	5,30 ± 1,23	-1,63 ± 1,26	-0,01 ± 0,08	-1,41 ± 0,73	2,25 ± 0,87
Asn 132	-0,29 ± 1,26	0,17 ± 1,33	0,00 ± 0,08	0,21 ± 0,72	0,09 ± 0,99
Glu 166	-15,17 ± 1,00	0,76 ± 1,32	0,02 ± 0,08	3,28 ± 0,52	-11,11 ± 0,87
Asn 170	-0,24 ± 1,26	0,88 ± 1,30	-0,01 ± 0,09	-1,38 ± 0,78	-0,75 ± 0,99
Val 216	-0,37 ± 1,89	0,75 ± 1,32	0,04 ± 0,08	-1,18 ± 1,15	-0,76 ± 1,29
Lys 234	13,95 ± 0,93	0,25 ± 1,33	-0,01 ± 0,08	-2,30 ± 0,52	11,89 ± 0,85
Ser 235	-0,06 ± 1,26	0,00 ± 1,33	0,00 ± 0,08	-0,12 ± 0,73	-0,18 ± 0,99
Glu 239	-7,57 ± 0,90	0,80 ± 1,28	0,15 ± 0,08	0,84 ± 0,52	-5,78 ± 0,83
Arg 244	7,55 ± 0,97	0,14 ± 1,32	0,01 ± 0,08	-0,74 ± 0,52	6,96 ± 0,86
Arg 275	5,18 ± 0,96	0,01 ± 1,33	0,00 ± 0,08	-0,69 ± 0,52	4,50 ± 0,86

Table 4. Decomposition of the Relative Binding Free Energy upon Computational ASM for Complex TEM-1/Amoxicillin

residues	amoxicillin/[kcal mol ⁻¹]				
	$\Delta\Delta E_{\text{Ele}} \pm \text{SD}$	$\Delta\Delta E_{\text{VDW}} \pm \text{SD}$	$\Delta\Delta G_{\text{nonpolar-solvation}} \pm \text{SD}$	$\Delta\Delta G_{\text{polar-solvation}} \pm \text{SD}$	$\Delta\Delta G_{\text{binding}} \pm \text{SD}$
Met 69	0,19 ± 1,91	0,25 ± 0,94	0,00 ± 0,06	-0,41 ± 1,10	0,03 ± 1,20
Ser 70	2,10 ± 1,22	0,23 ± 0,94	0,01 ± 0,06	-0,77 ± 0,70	1,57 ± 0,85
Lys 73	18,91 ± 0,83	-0,22 ± 0,94	-0,07 ± 0,06	-369 ± 0,69	14,93 ± 0,71
Tyr 105	0,06 ± 1,27	3,03 ± 0,89	0,29 ± 0,05	-1,02 ± 0,70	2,36 ± 0,85
Ser 130	-0,35 ± 1,32	0,04 ± 0,94	0,01 ± 0,06	0,33 ± 0,76	0,03 ± 0,90
Asn 132	-0,34 ± 1,40	2,04 ± 0,93	-0,05 ± 0,06	1,35 ± 0,85	3,00 ± 0,94
Glu 166	-12,98 ± 0,94	0,91 ± 0,94	-0,01 ± 0,06	7,22 ± 0,49	-4,86 ± 0,71
Asn 170	1,04 ± 1,28	2,18 ± 0,91	-0,05 ± 0,06	-1,26 ± 0,72	1,91 ± 0,87
Val 216	-0,47 ± 1,91	0,06 ± 0,94	0,01 ± 0,06	-0,28 ± 1,09	-0,68 ± 1,20
Lys 234	11,77 ± 0,88	0,13 ± 0,94	0,00 ± 0,05	-4,48 ± 0,54	7,42 ± 0,70
Ser 235	-0,10 ± 1,28	0,00 ± 0,94	0,00 ± 0,06	-0,14 ± 0,71	-0,24 ± 0,87
Glu 239	-3,56 ± 0,84	-0,81 ± 0,91	0,13 ± 0,05	2,71 ± 0,56	-1,53 ± 0,68
Arg 244	7,87 ± 0,95	0,04 ± 0,94	0,00 ± 0,06	-3,44 ± 0,53	4,47 ± 0,72
Arg 275	5,70 ± 0,97	0,02 ± 0,94	0,00 ± 0,06	-2,49 ± 0,51	3,23 ± 0,72

Table 5. Average Distances (Å) between Catalytic Residues through the MD Simulation

TEM-1			
$\chi \pm \sigma$	amoxicillin	ampicillin	itself
Ser70–Lys73	4,54 ± 1,31	5,96 ± 1,04	3,18 ± 0,75
Ser70–Ser130	4,46 ± 1,08	5,43 ± 1,00	4,90 ± 1,11
Lys73–Ser130	4,01 ± 1,22	5,46 ± 0,82	4,93 ± 0,64
Lys73–Glu166	2,95 ± 0,39	3,14 ± 0,52	4,39 ± 0,93

TEM-1/amoxicillin, distances lower than or equal to 4 Å are encountered 42.0% of the time, at which the proton transfer can occur (Figure 6).

The distance between Lys73–N ζ and Ser130–O γ also increases upon complex formation with ampicillin. It achieves values higher than 5 Å. Although the average distances are high, distances lower than 4 Å can still be found in TEM-1/ampicillin for 12.4% of the MD simulation (Figure 7). Therefore, the proton transfer is still viable. The TEM-1/amoxicillin complex presents an average of $4,01 \pm 1,22$, and 51.0% of the time, distances lower than 4 Å can be found.

The distance between Lys73–N ζ and Glu166–O ε in the complexes is lower than in TEM-1 alone, which is the result of the greater stability of this cluster after ligand binding and when compared to the other clusters studied in this work. According to

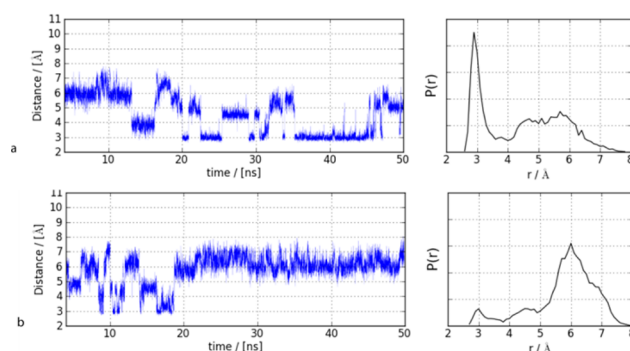


Figure 6. Graphical representation of the distance between Ser70–O γ and Lys73–N ζ during the MD simulation with the correspondent normalized distances⁹³ of the complexes of TEM-1 with amoxicillin (a) and ampicillin (b).

these results, TEM-1 can suffer readjustments of some residues within the catalytic pocket upon binding with the different antibiotics, suggesting that TEM-1 exhibits an induced fit of its ligands. This is supported not only by the differences observed between the uncomplexed TEM-1 and complexed TEM-1 but also with the differences observed between the complexes formed with ampicillin and amoxicillin. The distances between

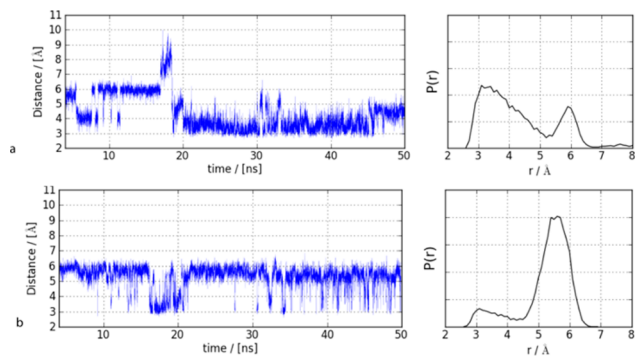


Figure 7. Graphical representation of the distance between Lys73–N ζ and Ser130–O γ during the MD simulation with the correspondent normalized distances⁹³ in complexes of TEM-1 with amoxicillin (a) and ampicillin (b).

key residues (Table 5) present significant differences between the complexes, and the HSs detected using ASM are also different. The acylation mechanism cannot be depicted here. However, it appears that this enzyme could be capable of acylating the antibiotics *via* an unsymmetrical mechanism (other proteases present an unsymmetrical catalytic mechanism) since the conserved water molecule responsible for the proton shuttle between Ser70 and Glu166 has been dislocated from its initial position upon Michaelis–Menten complex formation. This makes the water mediated proton transfer between these residues not viable, which avoids Ser70 activation. As discussed previously after acylation, the ligand presents the β -lactamic ring opened, and its position inside the catalytic pocket as well as its geometry should be different. These structural differences should allow for the relocation of some water molecules near the catalytic pocket such as the Glu166 and Ser70 bonded molecule that has been observed in pos-acylation crystallographic structures available in RCSB-PDB.¹⁰

CONCLUSION

In the complexes analyzed in this work, significant differences were detected. The interfacial residues of TEM-1 present different characteristics upon binding with the different ligands as the complexes with amoxicillin and ampicillin present different HSs. These results suggest that the effect of the ligand binding in each interfacial residue is not only dependent on its position and biochemical nature (charge, polarity, size) but also related with the chemical structure of the ligand. The orientation of the side chain of the residues is also different between the complexes and between these and TEM-1 uncomplexed. The differences observed with the calculation of the B-factor show that some residues near the catalytic pocket (Glu240) are more stable upon binding. Although this difference can be observed for both the backbone and side chain, it is more noticeable in the side chain, which is stabilized *via* interaction with the ligand. In all complexes, we observed a different distribution of the water molecules near the interfacial residues. The major one is the displacement of the catalytic water molecule that is highly conserved between Ser70 and Glu166 in several crystallographic structures. The position, orientation, and volume taken by the ligand in its intact form within the catalytic pocket are the most likely reasons for this finding, which would justify why this conserved water molecule can be found in structures only with TEM enzymes or pos-acylation. We have to highlight the possible adaptability shown by this enzyme that can only through

the displacement of the side chains of interfacial residues achieve noticeable differences between the various complexes.

ASSOCIATED CONTENT

S Supporting Information

The chemical structures of amoxicillin and ampicillin are shown in Figures S1, S2, and S3 with the atom names as labels in Figures S2 and S3. In Figure S4 are shown the complexes obtained with Molecular Docking superimposed with the complex TEM-1/penam from PDBID: 1FQG.⁷⁷ Atom names, atom types, and derived RESP charges for amoxicillin and ampicillin are appointed in Tables S1 and S3, respectively. In Tables S2 and S4 are depicted bond lengths and angle parameters derived with the HF/6-31G* level of theory for amoxicillin and ampicillin, respectively. Scheme 1 illustrates two of the proposed catalytic mechanisms for TEM-1, as described in the literature. This information is available free of charge via the Internet at <http://pubs.acs.org>.

AUTHOR INFORMATION

Corresponding Author

*E-mail: irina.moreira@fc.up.pt

Author Contributions

The manuscript was written through contributions of all authors. All authors have given approval to the final version of the manuscript.

Funding

I.S.M. is supported by FCT Ciéncia 2008 (Hiring of Ph.D.'s for the SCTN—financed by POPH—QREN—Typology 4.2—Promoting Scientific Employment, cofinanced by MES national funding and The European Social Fund).

Notes

The authors declare no competing financial interest.

REFERENCES

- (1) Bradford, P. A. Extended-spectrum beta-lactamases in the 21st century: characterization, epidemiology, and detection of this important resistance threat. *Clin. Microbiol. Rev.* **2001**, *14*, 933–951.
- (2) Bush, K.; Fisher, J. F. Epidemiological Expansion, Structural Studies, and Clinical Challenges of New beta-Lactamases from Gram-Negative Bacteria. *Annu. Rev. Microbiol.* **2011**, *65*, 455–478.
- (3) Wilke, M. S.; Lovering, A. L.; Strynadka, N. C. J. β -Lactam antibiotic resistance: a current structural perspective. *Curr. Opin. Microbiol.* **2005**, *8*, 525–533.
- (4) Jacoby, G. β -Lactamase Classification and Amino Acid Sequences for TEM, SHV and OXA Extended-Spectrum and Inhibitor Resistant Enzymes. <http://www.lahey.org/Studies/>.
- (5) Salverda, M. L.; De Visser, J. A.; Barlow, M. Natural evolution of TEM-1 β -lactamase: experimental reconstruction and clinical relevance. *FEMS Microbiol. Rev.* **2010**, *34*, 1015–1036.
- (6) Wang, X.; Minasov, G.; Shoichet, B. K. The structural bases of antibiotic resistance in the clinically derived mutant beta-lactamases TEM-30, TEM-32, and TEM-34. *J. Biol. Chem.* **2002**, *277*, 32149–32156.
- (7) Chaïbi, E. B.; Sirot, D.; Paul, G.; Labia, R. Inhibitor-resistant TEM beta-lactamases: phenotypic, genetic and biochemical characteristics. *J. Antimicrob. Chemother.* **1999**, *43*, 447–458.
- (8) Robin, F.; Delmas, J.; Schweitzer, C.; Tournilhac, O.; Lesens, O.; Chanal, C.; Bonnet, R. Evolution of TEM-type enzymes: biochemical and genetic characterization of two new complex mutant TEM enzymes, TEM-151 and TEM-152, from a single patient. *Antimicrob. Agents Chemother.* **2007**, *51*, 1304–1309.
- (9) Poirel, L.; Mammeri, H.; Nordmann, P. TEM-121, a novel complex mutant of TEM-type beta-lactamase from *Enterobacter aerogenes*. *Antimicrob. Agents Chemother.* **2004**, *48*, 4528–4531.

- (10) Bernstein, F. C.; Koetzle, T. F.; Williams, G. J.; Meyer, E. F.; Brice, M. D.; Rodgers, J. R.; Kennard, O.; Shimanouchi, T.; Tasumi, M. The Protein Data Bank. A computer-based archival file for macromolecular structures. *Eur. J. Biochem.* **1977**, *80*, 319–324.
- (11) Chandonia, J. M.; Brenner, S. E. The impact of structural genomics: expectations and outcomes. *Science* **2006**, *311*, 347–351.
- (12) Hunter, W. N. Present at the Flood. By Richard E. Dickerson. Sunderland, Mass.: Sinauer Associates, Inc., 2005. Pp. 307. ISBN 0-87893-168-6. *Acta Crystallogr., Sect. D: Biol. Crystallogr.* **2007**, *63*, 750.
- (13) Abola, E.; Kuhn, P.; Earnest, T.; Stevens, R. C. Automation of X-ray crystallography. *Nat. Struct. Biol.* **2000**, *7*, 973–977.
- (14) Sorensen, T. L.; McAuley, K. E.; Flraig, R.; Duke, E. M. New light for science: synchrotron radiation in structural medicine. *Trends Biotechnol.* **2006**, *24*, 500–508.
- (15) Marco, E.; Gago, F. Overcoming the Inadequacies or Limitations of Experimental Structures as Drug Targets by Using Computational Modeling Tools and Molecular Dynamics Simulations. *ChemMedChem* **2007**, *2*, 1388–1401.
- (16) Moreira, I. S.; Martins, J. M.; Ramos, R. M.; Fernandes, P. A.; Ramos, M. J. Understanding the importance of the aromatic amino-acid residues as hot-spots. *Biochim. Biophys. Acta, Proteins Proteomics* **2013**, *1834*, 404–414.
- (17) Gerstein, M.; Krebs, W. A database of macromolecular motions. *Nucleic Acids Res.* **1998**, *26*, 4280–4290.
- (18) Oliveira, B. L.; Moreira, I. S.; Fernandes, P. A.; Ramos, M. J.; Santos, I.; Correia, J. D. Insights into the structural determinants for selective inhibition of nitric oxide synthase isoforms. *J. Mol. Model.* **2012**, *19*, 1537–1551.
- (19) Karplus, M.; McCammon, J. A. Molecular dynamics simulations of biomolecules. *Nat. Struct. Mol. Biol.* **2002**, *9*, 646–652.
- (20) Martins, J. M.; Ramos, R. M.; Moreira, I. S. Structural determinants of a typical leucine-rich repeat protein. *Commun. Comput. Phys.* **2013**, *13*, 238–255.
- (21) Moreira, I. S.; Fernandes, P. A.; Ramos, M. J. Hot spot occlusion from bulk water: a comprehensive study of the complex between the lysozyme HEL and the antibody FVD1.3. *J. Phys. Chem. B* **2007**, *111*, 2697–2706.
- (22) Moreira, I. S.; Fernandes, P. A.; Ramos, M. J. Detailed microscopic study of the full ZipA: FtsZ interface. *Proteins: Struct., Funct., Bioinf.* **2006**, *63*, 811–821.
- (23) Durrant, J.; McCammon, J. A. Molecular dynamics simulations and drug discovery. *BMC Biol.* **2011**, *9*, 71.
- (24) Fisette, O.; Morin, S.; Savard, P. Y.; Lagüe, P.; Gagné, S. M. TEM-1 backbone dynamics-insights from combined molecular dynamics and nuclear magnetic resonance. *Biophys. J.* **2010**, *98*, 637–645.
- (25) Bös, F.; Pleiss, J. Multiple molecular dynamics simulations of TEM beta-lactamase: dynamics and water binding of the omega-loop. *Biophys. J.* **2009**, *97*, 2550–2558.
- (26) Díaz, N.; Suárez, D.; Merz, K. M.; Sordo, T. L. Molecular dynamics simulations of the TEM-1 beta-lactamase complexed with cephalothin. *J. Med. Chem.* **2005**, *48*, 780–791.
- (27) Stec, B.; Holtz, K. M.; Wojciechowski, C. L.; Kantrowitz, E. R. Structure of the wild-type TEM-1 beta-lactamase at 1.55 Å and the mutant enzyme Ser70Ala at 2.1 Å suggest the mode of noncovalent catalysis for the mutant enzyme. *Acta Crystallogr., Sect. D: Biol. Crystallogr.* **2005**, *61*, 1072–1079.
- (28) Thomas, V. L.; Golemi-Kotra, D.; Kim, C.; Vakulenko, S. B.; Mobashery, S.; Shoichet, B. K. Structural consequences of the inhibitor-resistant Ser130Gly substitution in TEM beta-lactamase. *Biochemistry* **2005**, *44*, 9330–9338.
- (29) Saves, I.; Burlet-Schiltz, O.; Swarén, P.; Lefèvre, F.; Masson, J. M.; Promé, J. C.; Samama, J. P. The asparagine to aspartic acid substitution at position 276 of TEM-35 and TEM-36 is involved in the beta-lactamase resistance to clavulanic acid. *J. Biol. Chem.* **1995**, *270*, 18240–18245.
- (30) Thorsen, T. S.; Madsen, K. L.; Rebola, N.; Rathje, M.; Anggono, V.; Bach, A.; Moreira, I. S.; Stuhr-Hansen, N.; Dyhring, T.; Peters, D.; Beuming, T.; Huganir, R.; Weinstein, H.; Mulle, C.; Strømgaard, K.; Rønne, L. C.; Gether, U. Identification of a small-molecule inhibitor of the PICK1 PDZ domain that inhibits hippocampal LTP and LTD. *Proc. Natl. Acad. Sci. U. S. A.* **2010**, *107*, 413–418.
- (31) Bach, A.; Stuhr-Hansen, N.; Thorsen, T. S.; Bork, N.; Moreira, I. S.; Frydenvang, K.; Padrah, S.; Christensen, S. B.; Madsen, K. L.; Weinstein, H.; Gether, U.; Strømgaard, K. Structure-activity relationships of a small-molecule inhibitor of the PDZ domain of PICK1. *Org. Biomol. Chem.* **2010**, *8*, 4281–4288.
- (32) Ramamoorthy, D.; Turos, E.; Guida, W. C. Identification of a New Binding Site in *E. coli* FabH using Molecular Dynamics Simulations: Validation by Computational Alanine Mutagenesis and Docking Studies. *J. Chem. Inf. Model.* **2013**, *53*, 1138–1156.
- (33) Lee, H. S.; Jo, S.; Lim, H.-S.; Im, W. Application of Binding Free Energy Calculations to Prediction of Binding Modes and Affinities of MDM2 and MDMX Inhibitors. *J. Chem. Inf. Model.* **2012**, *52*, 1821–1832.
- (34) De Luca, L.; Morreale, F.; Chimirri, A. Insight into the Fundamental Interactions between LEDGF Binding Site Inhibitors and Integrase Combining Docking and Molecular Dynamics Simulations. *J. Chem. Inf. Model.* **2012**, *52*, 3245–3254.
- (35) Moreira, I. S.; Fernandes, P. A.; Ramos, M. J. Hot spots-A review of the protein-protein interface determinant amino-acid residues. *Proteins: Struct., Funct., Bioinf.* **2007**, *68*, 803–812.
- (36) Shelley, J.; Cholleti, A.; Frye, L.; Greenwood, J.; Timlin, M.; Uchimaya, M. Epik: a software program for pK a prediction and protonation state generation for drug-like molecules. *J. Comput.-Aided Mol. Des.* **2007**, *21*, 681–691.
- (37) Maestro, version 9.2; Schrödinger, Inc.; New York, 2011.
- (38) Cornell, W. D.; Cieplak, P.; Bayly, C. I.; Gould, I. R.; Merz, K. M.; Ferguson, D. M.; Spellmeyer, D. C.; Fox, T.; Caldwell, J. W.; Kollman, P. A. A Second Generation Force Field for the Simulation of Proteins, Nucleic Acids, and Organic Molecules. *J. Am. Chem. Soc.* **1995**, *117*, 5179–5197.
- (39) Duan, Y.; Wu, C.; Chowdhury, S.; Lee, M. C.; Xiong, G.; Zhang, W.; Yang, R.; Cieplak, P.; Luo, R.; Lee, T.; Caldwell, J.; Wang, J.; Kollman, P. A point-charge force field for molecular mechanics simulations of proteins based on condensed-phase quantum mechanical calculations. *J. Comput. Chem.* **2003**, *24*, 1999–2012.
- (40) Berendsen, H. J. C.; Postma, J. P. M.; van Gunsteren, W. F.; DiNola, A.; Haak, J. R. Molecular dynamics with coupling to an external bath. *J. Chem. Phys.* **1984**, *81*, 3684–3690.
- (41) Ryckaert, J.-P.; Ciccotti, G.; Berendsen, H. J. C. Numerical integration of the cartesian equations of motion of a system with constraints: molecular dynamics of n-alkanes. *J. Comput. Phys.* **1977**, *23*, 327–341.
- (42) Loncharich, R. J.; Brooks, B. R.; Pastor, R. W. Langevin dynamics of peptides: The frictional dependence of isomerization rates of N-acetylalanyl-N'-methylamide. *Biopolymers* **1992**, *32*, 523–535.
- (43) Izaguirre, J. A.; Catarello, D. P.; Woźniak, J. M.; Skeel, R. D. Langevin stabilization of molecular dynamics. *J. Chem. Phys.* **2001**, *114*, 2090–2098.
- (44) Ewald, P. P. Die Berechnung optischer und elektrostatischer Gitterpotentiale. *Ann. Phys. (Berlin, Ger.)* **1921**, *369*, 253–287.
- (45) Darden, T.; York, D.; Pedersen, L. Particle mesh Ewald: An N [center-dot] log(N) method for Ewald sums in large systems. *J. Chem. Phys.* **1993**, *98*, 10089–10092.
- (46) Bush, K.; Jacoby, G. A. Updated functional classification of beta-lactamases. *Antimicrob. Agents Chemother.* **2010**, *54*, 969–976.
- (47) Suárez, C. Antibióticos betalactámicos. *Enferm. Infect. Microbiol. Clin.* **2009**, *27*, 116–129.
- (48) Bolton, E. E.; Wang, Y.; Thiessen, P. A.; Bryant, S. H., Chapter 12 PubChem: Integrated Platform of Small Molecules and Biological Activities. In *Annu. Rep. Comput. Chem.*; Ralph, A. W. a. D. C. S., Ed.; Elsevier: New York, 2008; Vol. 4, pp 217–241.
- (49) Morris, G. M.; Huey, R.; Lindstrom, W.; Sanner, M. F.; Belew, R. K.; Goodsell, D. S.; Olson, A. J. AutoDock4 and AutoDockTools4: Automated docking with selective receptor flexibility. *J. Comput. Chem.* **2009**, *30*, 2785–2791.
- (50) Bayly, C. I.; Cieplak, P.; Cornell, W.; Kollman, P. A. A well-behaved electrostatic potential based method using charge restraints for

- deriving atomic charges: the RESP model. *J. Chem. Phys.* **1993**, *97*, 10269–10280.
- (51) Case, D. A.; Cheatham, T. E.; Darden, T.; Gohlke, H.; Luo, R.; Merz, K. M.; Onufriev, A.; Simmerling, C.; Wang, B.; Woods, R. J. The Amber biomolecular simulation programs. *J. Comput. Chem.* **2005**, *26*, 1668–1688.
- (52) Wang, J.; Wolf, R. M.; Caldwell, J. W.; Kollman, P. A.; Case, D. A. Development and testing of a general amber force field. *J. Comput. Chem.* **2004**, *25*, 1157–1174.
- (53) Stapleton, P. D.; Shannon, K. P.; French, G. L. Construction and characterization of mutants of the TEM-1 beta-lactamase containing amino acid substitutions associated with both extended-spectrum resistance and resistance to beta-lactamase inhibitors. *Antimicrob. Agents Chemother.* **1999**, *43*, 1881–1887.
- (54) Knox, J. R. Extended-spectrum and inhibitor-resistant TEM-type beta-lactamases: mutations, specificity, and three-dimensional structure. *Antimicrob. Agents Chemother.* **1995**, *39*, 2593–2601.
- (55) Humphrey, W.; Dalke, A.; Schulten, K. VMD: Visual molecular dynamics. *J. Mol. Graphics* **1996**, *14*, 33–38.
- (56) DeLano, W. L. *The PyMOL Molecular Graphics System*; DeLano Scientific: San Carlos, CA, 2002.
- (57) Huo, S.; Massova, I.; Kollman, P. A. Computational alanine scanning of the 1: 1 human growth hormone-receptor complex. *J. Comput. Chem.* **2002**, *23*, 15–27.
- (58) Case, D. A.; Darden, T. A.; Cheatham, T. E., III; Simmerling, C. L.; Wang, J.; Duke, R. E.; Luo, R.; Crowley, M.; Walker, R. C.; Zhang, W.; Merz, K. M.; Wang, B.; Hayik, S.; Roitberg, A.; Seabra, G.; Kolossvary, I.; Wong, K. F.; Paesani, F.; Vanicek, J.; Wu, X.; Brozell, S. R.; Steinbrecher, T.; Gohlke, H.; Yang, L.; Tan, C.; Mongan, J.; Hornak, V.; Cui, G.; Mathews, D. H.; Seetin, M. G.; Sagui, C.; Babin, V.; Kollman, P. A. AMBER 10; University of California: San Francisco, CA, 2008.
- (59) Moreira, I. S.; Fernandes, P. A.; Ramos, M. J. Unraveling the importance of protein-protein interaction: Application of a computational alanine-scanning mutagenesis to the study of the IgG1 streptococcal protein G (C2 fragment) complex. *J. Phys. Chem. B.* **2006**, *110*, 10962–10969.
- (60) Moreira, I. S.; Fernandes, P. A.; Ramos, M. J. Unravelling Hot Spots: a comprehensive computational mutagenesis study. *Theor. Chem. Acc.* **2007**, *117*, 99–113.
- (61) Moreira, I. S.; Fernandes, P. A.; Ramos, M. J. Hot spot computational identification: Application to the complex formed between the hen egg white lysozyme (HEL) and the antibody HyHEL-10. *Int. J. Quantum Chem.* **2007**, *107*, 299–310.
- (62) Moreira, I. S.; Fernandes, P. A.; Ramos, M. J. Computational alanine scanning mutagenesis - An improved methodological approach. *J. Comput. Chem.* **2007**, *28*, 644–654.
- (63) Moreira, I. S.; Fernandes, P. A.; Ramos, M. J. Backbone importance for protein-protein binding. *J. Chem. Theory Comput.* **2007**, *3*, 885–893.
- (64) Moreira, I. S.; Fernandes, P. A.; Ramos, M. J. Hot spot occlusion from bulk water: A comprehensive study of the complex between the lysozyme HEL and the antibody FVD1.3. *J. Phys. Chem. B* **2007**, *111*, 2697–2706.
- (65) Moreira, I. S.; Fernandes, P. A.; Ramos, M. J. Protein-protein recognition: a computational mutagenesis study of the MDM2-P53 complex. *Theor. Chem. Acc.* **2008**, *120*, 533–542.
- (66) Chong, L. T.; Duan, Y.; Wang, L.; Massova, I.; Kollman, P. A. Molecular dynamics and free-energy calculations applied to affinity maturation in antibody 48G7. *Proc. Natl. Acad. Sci. U. S. A.* **1999**, *96*, 14330–14335.
- (67) Kollman, P. A.; Massova, I.; Reyes, C.; Kuhn, B.; Huo, S. H.; Chong, L.; Lee, M.; Lee, T.; Duan, Y.; Wang, W.; Donini, O.; Cieplak, P.; Srinivasan, J.; Case, D. A.; Cheatham, T. E. Calculating structures and free energies of complex molecules: Combining molecular mechanics and continuum models. *Acc. Chem. Res.* **2000**, *33*, 889–897.
- (68) Bradshaw, R. T.; Patel, B. H.; Tate, E. W.; Leatherbarrow, R. J.; Gould, I. R. Comparing experimental and computational alanine scanning techniques for probing a prototypical protein-protein interaction. *Protein Eng., Des. Sel.* **2011**, *24*, 197–207.
- (69) Moreira, I. S.; Martins, J. M.; Ramos, M. J.; Fernandes, P. A.; Ramos, M. J. Understanding the importance of the aromatic amino-acid residues as hot-spots. *Biochem. Biophys. Acta.* **2013**, *1834*, 401–414.
- (70) Ribeiro, J. V.; Cerqueira, N. M. F. S. A.; Moreira, I. S.; Fernandes, P. A.; Ramos, M. J. CompASM: an Amber-VMD Alanine Scanning Mutagenesis plug-in. *Theor. Chem. Acc.* **2012**, *131*, 1271–1278.
- (71) Rocchia, W.; Alexov, E.; Honig, B. Extending the applicability of the nonlinear Poisson-Boltzmann equation: Multiple dielectric constants and multivalent ions. *J. Phys. Chem. B.* **2001**, *105*, 6507–6514.
- (72) Rocchia, W.; Sridharan, S.; Nicholls, A.; Alexov, E.; Chiabrera, A.; Honig, B. Rapid grid-based construction of the molecular surface and the use of induced surface charge to calculate reaction field energies: Applications to the molecular systems and geometric objects. *J. Comput. Chem.* **2002**, *23*, 128–137.
- (73) Moreira, I. S.; Fernandes, P. A.; Ramos, M. J. Accuracy of the numerical solution of the Poisson-Boltzmann equation. *J. Mol. Struct.: THEOCHEM* **2005**, *729*, 11–18.
- (74) Sitkoff, D.; Sharp, K. A.; Honig, B. Accurate calculation of hydration free-energies using macroscopic solvent models. *J. Phys. Chem.* **1994**, *98*, 1978–1988.
- (75) Connolly, M. L. Analytical molecular surface calculation. *J. Appl. Crystallogr.* **1983**, *16*, 548–558.
- (76) Konc, J.; Janežič, D. ProBiS-2012: web server and web services for detection of structurally similar binding sites in proteins. *Nucleic Acids Res.* **2012**, *40*, W214–221.
- (77) Strynadka, N. C.; Adachi, H.; Jensen, S. E.; Johns, K.; Sielecki, A.; Betzel, C.; Sutoh, K.; James, M. N. Molecular structure of the acyl-enzyme intermediate in beta-lactam hydrolysis at 1.7 Å resolution. *Nature* **1992**, *359*, 700–705.
- (78) Maveyraud, L.; Massova, I.; Birck, C.; Miyashita, K.; Samama, J. P.; Mobashery, S. Crystal Structure of 6Alpha-Hydroxymethylpenicillinate Complexed to the Tem-1 Beta-Lactamase from Escherichia Coli: Evidence on the Mechanism of Action of a Novel Inhibitor Designed by a Computer-Aided Process. *J. Am. Chem. Soc.* **1996**, *118*, 7435.
- (79) Maveyraud, L.; Mourey, L.; Kotra, L. P.; Pedelacq, J.-D.; Guillet, V.; Mobashery, S.; Samama, J.-P. Structural Basis for Clinical Longevity of Carbapenem Antibiotics in the Face of Challenge by the Common Class A β-Lactamases from the Antibiotic-Resistant Bacteria. *J. Am. Chem. Soc.* **1998**, *120*, 9748–9752.
- (80) Roccatano, D.; Sbardella, G.; Aschi, M.; Amicosante, G.; Bossa, C.; Di Nola, A.; Mazza, F. Dynamical aspects of TEM-1 beta-lactamase probed by molecular dynamics. *J. Comput.-Aided Mol. Des.* **2005**, *19*, 329–340.
- (81) Massova, I.; Kollman, P. A. pKa, MM, and QM studies of mechanisms of β-lactamases and penicillin-binding proteins: Acylation step. *J. Comput. Chem.* **2002**, *23*, 1559–1576.
- (82) Medeiros, A. A. Evolution and dissemination of beta-lactamases accelerated by generations of beta-lactam antibiotics. *Clin. Infect. Dis.* **1997**, *24* (Suppl 1), S19–45.
- (83) Matagne, A.; Lamotte-Brasseur, J.; Frère, J. M. Catalytic properties of class A beta-lactamases: efficiency and diversity. *Biochem. J.* **1998**, *330* (Pt 2), 581–598.
- (84) Bren, U.; Oostenbrink, C. Cytochrome P450 3A4 inhibition by ketoconazole: tackling the problem of ligand cooperativity using molecular dynamics simulations and free-energy calculations. *J. Chem. Inf. Model.* **2012**, *52*, 1573–1582.
- (85) Bren, U.; Janežič, D. Individual degrees of freedom and the solvation properties of water. *J. Chem. Phys.* **2012**, *137*, 024108.
- (86) Bren, U.; Krzan, A.; Mavri, J. Microwave catalysis through rotationally hot reactive species. *J. Phys. Chem. A.* **2008**, *112*, 166–171.
- (87) Hamza, A.; Abdulhameed, M. D.; Zhan, C. G. Understanding microscopic binding of human microsomal prostaglandin E synthase-1 with substrates and inhibitors by molecular modeling and dynamics simulation. *J. Phys. Chem. B.* **2008**, *112*, 7320–7329.
- (88) Dubey, K. D.; Ojha, R. P. Binding free energy calculation with QM/MM hybrid methods for Abl-Kinase inhibitor. *J. Biol. Phys.* **2011**, *37*, 69–78.

- (89) Bren, M.; Florián, J.; Mavri, J.; Bren, U. Do all pieces make a whole? Thiele cumulants and the free energy decomposition. *Theor. Chem. Acc.* **2007**, *117*, 535–540.
- (90) Bogan, A. A.; Thorn, K. S. Anatomy of hot spots in protein interfaces. *J. Mol. Biol.* **1998**, *280*, 1–9.
- (91) Moreira, I. S.; Ramos, R. M.; Martins, J. M.; Fernandes, P. A.; Ramos, M. J., Are hot-spots occluded from water? *J. Biomol. Struct. Dyn.* **2013**, [Online] http://www.tandfonline.com/doi/abs/10.1080/07391102.2012.758598?url_ver=Z39.88-2003&rfr_id=ori:rid:crossref.org&rfr_dat=cr_pub%3dpubmed#.UfKusvkqeSo (accessed July 26, 2013).
- (92) Nejc, C.; Hodošček, M.; Vehar, B.; Konc, J.; Brooks, B. R.; Janežič, D. Correlating Protein Hot Spot Surface Analysis Using ProBiS with Simulated Free Energies of Protein–Protein Interfacial Residues. *J. Chem. Inf. Model.* **2012**, *52*, 2541–2549.
- (93) Graf, M. M.; Bren, U.; Haltrich, D.; Oostenbrink, C. Molecular dynamics simulations give insight into D-glucose dioxydation at C2 and C3 by Agaricus meleagris pyranose dehydrogenase. *J. Comput.-Aided Mol. Des.* **2013**, *27*, 295–304.